Mass spectrometric determination of partial electron impact ionization cross sections of He, Ne, Ar and Kr from threshold up to 180 eV

K. Stephan, H. Helm,[a] and T. D. Märk

Abteilung für Kernphysik und Gaselektronik, Institut für Experimentalphysik, Leopold Franzens Universität, A-6020 Innsbruck, Österreich, Austria
(Received 12 May 1980; accepted 19 June 1980)

A new approach to mass spectrometric measurement and analysis has been used to study the electron impact ionization of the rare gases in the low electron energy regime (< 180 eV). Critical considerations are given to the problems of ion extraction from the ion source (Nier-type) and the transmission of the extracted ions through the mass spectrometer system (double focusing sector field Varian MAT CH5). Accurate relative partial cross section functions were obtained for production of He^+ and He^{2+} from He; Ne^+, Ne^{2+}, and Ne^{3+} from Ne; Ar^+, Ar^{2+}, Ar^{3+} from Ar, and Kr^+, Kr^{2+}, Kr^{3+} and Kr^{4+} from Kr. In addition, the cross section ratios for the partial ionization cross sections of each individual gas were determined. These ratios were used to sum up the relative partial cross section functions for each gas, hence obtaining relative total ionization cross section functions by weighting each partial cross section function with the respective charge number. The shape of the relative total ionization cross section function thus obtained was compared with ionization tube measurements of the total ionization cross section curve. Good agreement with the data of Rapp and Englander-Golden was found. This comparison allows the normalization of the measured relative partial cross section functions, yielding absolute partial cross section values for all of the processes mentioned above. The experimental results presented are compared with previous determinations where available.

I. INTRODUCTION

Experimental data concerning the electron impact ionization of atoms and molecules are of great importance in the physics and chemistry of ionized gases. The conceptual simplicity of the experimental techniques used for the determination of electron impact ionization cross sections, unfortunately, by no means implies that such measurements are easy and/or will be reliable.[1] The situation is especially difficult if partial ionization cross sections [partial ionization cross sections are defined here as cross sections describing the electron impact production of an ion of specific charge n, e.g., $e + Y \rightarrow Y^{n+} + (n+1)e$] are to be measured. In this case a mass spectrometer must be used for the analysis, but, according to Kieffer and Dunn,[1] in general the assumption of a constant collection efficiency for the different ions observed has not been proved by previous authors.

Even for the atomic rare gases, large differences exist in magnitude[1,2] and in shape[1,3,4] of experimentally determined partial ionization cross section functions measured by different authors. Despite the importance of the rare gases, not counting the numerous papers on the threshold behavior of the cross sections, only a few mass spectrometric studies have been made on single and multiple electron impact ionization in the low electron energy regime (< 200 eV).[1,2] Most of the previous studies have been concerned with the investigation of relative partial ionization cross section functions in only one or two rare gases, or have been restricted to the measurement of cross section ratios at one particular electron energy. Also, some of the relative abundances of multiply charged ions have been measured using electron multipliers as detectors. However, these have not taken proper account of different secondary electron emission coefficients for different ions.

The first quantitative electron impact ionization experiments with rare gases date back to the early 1930's and were performed by Bleakney,[5] Tate and Smith,[6] Bleakney and Smith,[7] and Stevenson and Hipple.[8] This early work had been repeated in only a few instances (see Ref. 1 and 2), but in general the new measurements (with a few exceptions[9–11]) not being any extension or improvement over the earlier data.[5–8] Hence, the results of these authors[5–8] have remained as standards ever since.[1] In the last few years we have set about repeating and extending the work of the early partial cross section measurements in order to obtain more accurate information about the electron impact formation of singly and multiply charged rare gas ions. This has led to several studies of the properties of an electron impact ion source mass spectrometer system.[12–22] The present paper reports a new approach to mass spectrometric measurement and analysis, where emphasis is placed on consistency checks to ensure controlled extraction and collection of ions, and on demonstrating that the measured relative partial ionization cross section functions are independent of instrumental errors. Because of these improvements and precautions, we believe that the reported energy dependence of partial ionization cross sections and the cross section ratios are highly accurate. The absolute calibration of relative partial cross sections is a difficult experimental task, for which we have not yet found a satisfactory experimental approach. In the current paper we normalize the weighted sum of the relative partial cross sections determined at one particular electron energy to the values of the total ionization cross sections reported by Rapp and Englander-Golden.[23] The normalization fac-

[a]Current address: Molecular Physics Laboratory, SRI International, Menlo Park, Cal. 94025.

 0021-9606/80/203763-16$01.00

tors for the total ionization cross sections are found to be independent of electron energy within the limits of experimental error. This lends further credibility to the energy dependence of the partial ionization cross section functions measured in the present study. Results reported presently include the following for He, Ne, Ar, and Kr: (1) relative partial ionization cross section functions, (2) ratios of partial cross sections, and (3) absolute partial ionization cross sections obtained by the aforementioned normalization procedure. The range of the electron energy covered is from threshold up to 180 eV. The paper also contains a discussion of previous data.

II. EXPERIMENTAL

A. Apparatus

The apparatus used in the present study is basically the same as that used previously for studying the electron impact ionization of various molecules.[24] However, for the present set of measurements some experimental details and the mode of ion source operation were changed. Figure 1 gives a schematic view of the ion source–mass spectrometer setup (Varian MAT CH5). One of the experimental modifications is an additional pair of deflection plates L_8, L_9. The ion beam leaving the ion source is shown schematically in order to demonstrate that under the usual operating conditions only a small fraction of the ion beam can enter the double focusing sector field mass analyzer through the entrance slit S_1. The mass analyzed ion beam passes the exit slit S_2 and then a shielding grid before striking the first dynode of an electron multiplier. A Faraday cup collector can be inserted between the shielding grid and the multiplier to measure the mass analyzed ion signal directly. The width of the slits S_1 and S_2 can be changed continuously.

Figure 2 shows the electron ion source in detail.

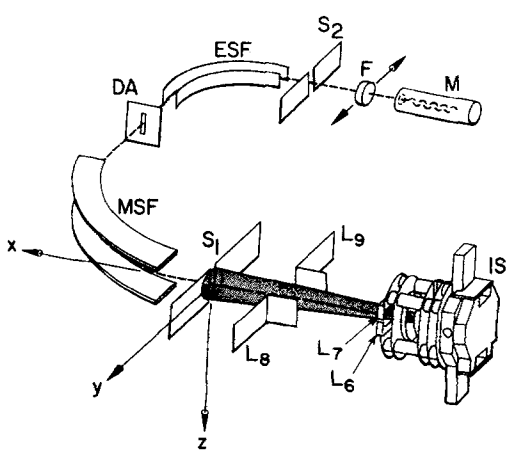

FIG. 1. Schematic illustration of the double focusing sector field mass spectrometer and the Nier-type ion source. MSF: 90° magnetic sector field; ESF: 90° electric sector field; IS: Nier-type ion source (see Fig. 2); S_1: mass spectrometer entrance slit; S_2: mass spectrometer exit slit; DA: defining aperture; F: Faraday collector; M: electron multiplier; $L_{6,7}$: z-deflection electrodes; L_8, L_9: y-deflection electrodes.

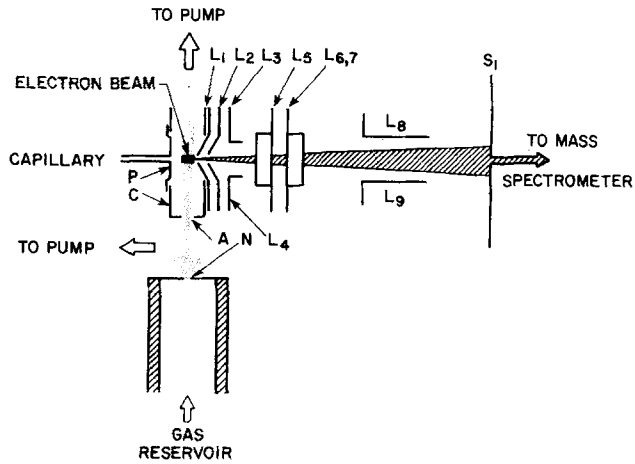

FIG. 2. Schematic view of electron impact ion source. P: pusher; C: collision chamber; CL: capillary leak; A: aperture; N: nozzle (10 to 50 μm diameter); L_1: collision chamber exit slit electrode; L_2 to L_5: ion beam focusing and accelerating electrodes; $L_{6,7}$ and $L_{8,9}$: z- and y-deflection electrodes; S_1: mass spectrometer entrance slit.

After bakeout, a background pressure of several 10^{-7} Torr is reached in the ion source vessel. The gas can be introduced into the ion source either directly via a capillary leak, resulting in a static gas target which uniformly fills the collision chamber, or via a flow nozzle, resulting in a molecular beam.[25] The rare gases used were spectroscopically pure laboratory gases from Linde.

The nozzle N is 10 to 50 μm in diameter and a fraction of the emerging beam enters the collision chamber C through a 5 mm diameter aperture A which is situated approximately 20 mm downstream from the nozzle. In this case, the target gas in the collision chamber consists partly of unscattered beam particles, and partly of gas particles which have been backscattered from the walls. At the highest inlet gas pressures used, the background pressure in the ion source chamber reaches typically 10^{-5} Torr. The temperature of the collision chamber can be controlled between 100 and 250 °C; most of the measurements were performed at a constant temperature of 250 °C.

During the course of earlier work,[12–22,24] some of the operating conditions of this commercial ion source (Varian MAT Intensitron M) have been improved. First, the electron trap potential was raised from 7 to 24 V. Second, the range of the continuously selectable electron accelerating voltage was expanded to vary from 5 V up to 180 V (current ranges selectable from 0.1 μA to 1 mA). In addition, measurement of partial ionization cross sections as a function of electron energy also requires the measurement of the electron current responsible for the ionization. It was found that a fraction of the electron current transversing the collision chamber *strikes* the electron exit slit (EES in Fig. 3) due to the angular divergence of the electron beam. This current is designated as stray electron current i_s. Figure 4 shows the dependence of the stray electron current i_s to trap current (current on T in Fig. 3) i_t as a function of the Wehnelt cylinder potential (the parameters in Fig. 4

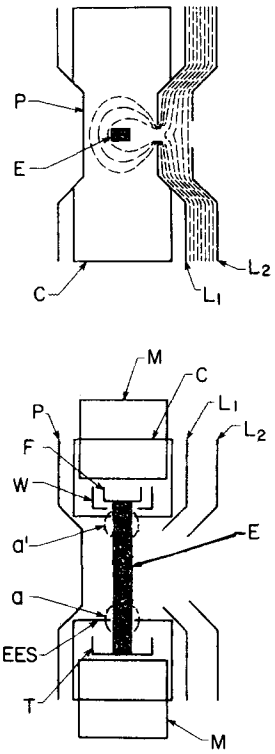

FIG. 3. Schematic diagram of equipotentials in the ion source for ion extraction by means of a penetrating field fringing into the collision chamber from the gap in L_1. C: collision chamber; P: pusher; F: filament; W: Wehnelt cylinder; EES: electron exit slit; E: electron beam; M: guiding magnet (magnetic field ≈ 40 mT); L_1: collision chamber exit electrodes; L_2: focusing electrodes; a and a' define the ion withdrawal space.

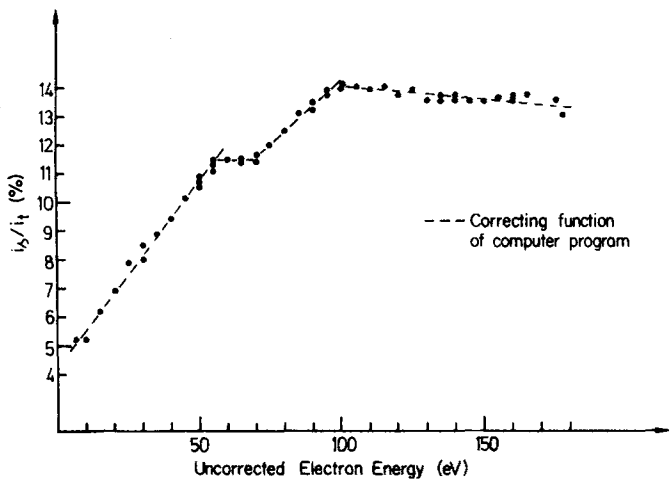

FIG. 5. The ratio between electron stray current and electron trap current i_s/i_t versus uncorrected electron energy for a constant electron trap current of 3 μA.

are the potential difference U_{tc} between electron trap T and collision chamber EES, and the electron energy). It was found that this ratio also depends on the filament current. From Fig. 4 it follows that the potential of the electron focusing Wehnelt cylinder should be maintained proportionally to the electron accelerating voltage in order to keep the stray electron current over the entire electron energy range as small as possible for a chosen U_{tc}. (A value of U_{tc} equal to 24 V was chosen in order to minimize the penetration of this field into the collision chamber.) Under these operating conditions it was possible to keep the electron stray current below 14% of the electron trap current (for electron currents $\lesssim 3$ μA)

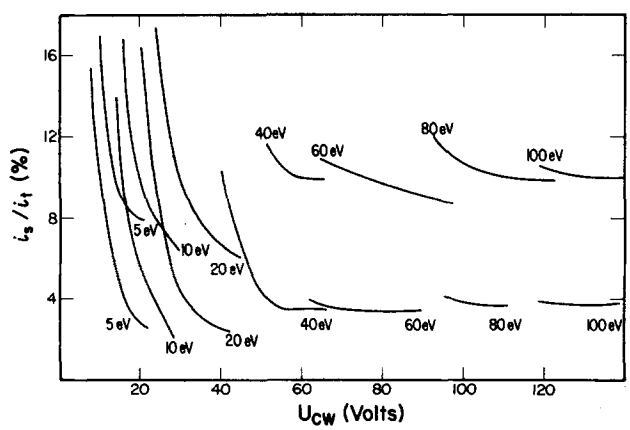

FIG. 4. The ratio between electron stray current i_s and electron trap current i_t versus the potential difference between collision chamber and Wehnelt cylinder at a filament current of 4 A and various electron energies. The lower group of curves corresponds to an electron trap collector potential of 70 V, whereas the upper group of curves corresponds to 24 V.

over the entire energy range. The measured ratio i_s/i_t is shown in Fig. 5 as a function of electron energy. During measurements of partial ionization cross sections, the electron trap current was monitored continuously, whereby the total electron current available for ionization in the collision chamber could be determined from the dependence shown in Fig. 5. Using a retarding potential technique, the energy spread (FWHM) in the electron beam was found to be approximately 500 mV.

B. Experimental technique and consistency checks

Because of the difficulty in measuring the absolute gas density in the collision chamber, and the difficulty in determining the collection efficiency of an ion source–mass spectrometer system, the primary value of mass spectrometric studies of partial ionization cross sections is the determination of relative partial ionization cross sections as a function of electron energy $q(E)$ or the determination of cross section ratios $q_n(E)/q_1(E)$. It is necessary to show that the ion collection efficiency is independent of $m/n \cdot e$ and of the electron energy (m is the mass of the ion and e is the electric charge).

Hence, we have studied the influence of (1) gas density and temperature in the collision chamber, (2) extraction field, (3) ion beam focusing conditions, (4) electron current and energy, and (5) the guiding magnetic field on the extraction characteristics of the ion source and on the observed relative partial ionization cross section functions and ratios. Based on this information[14,19,20,22,25] it was possible to devise a mode of ion source operation for which independence of the ion collection efficiency on $m/n \cdot e$ and the electron energy could be achieved.

A survey of previous studies on rare gas electron impact ionization and/or on mass spectrometer discrimination effects with similar ion source–mass spectrometer systems revealed that in many cases the ions are drawn from a region in which there is a crossed electric and magnetic field. In some cases[5–8,28–29] the source region is in the same uniform magnetic field that is used to analyze the ions. In other cases an auxiliary magnet-

ic field, supplied by a small permanent magnet, is used to collimate the electron beam. The electric field used for the extraction of ions[2,5-8,11,26-43] is in most cases a weak field applied between the collision chamber exit slit and an electrode opposite to the exit slit (called pusher or repeller), or between the exit slit and the collision chamber. Superimposed on this extraction field is, in most cases, a penetrating field from lenses beyond the extraction lens L_1,[37] which forms the collision chamber exit slit. It has been pointed out that ion sources operated in such a way discriminate against ions having different initial kinetic energies and/or mass to charge ratio.[27-29,33,34,36,39,43-45] Attempts to study the ion optical properties of such a Nier type ion source, in particular the influence of the repeller voltage on the ion trajectories, have been made.[35,40,41,45-47] Also, discrimination in the region between the ion source and detector due to initial velocity components parallel to the magnetic field scattering ions out of the ion beam has been discussed.[28,43,44] The discrimination at the mass spectrometer exit slit was eliminated with the help of deflecting electrodes immediately behind the mass spectrometer entrance slit.[11,28,43] Nevertheless, it has been demonstrated that, even for ions having thermal energies initially, measured ion currents and/or relative abundances strongly depend on the geometry of such an ion source system, and on the accelerating voltages applied.

In a second approach the electric field necessary to extract the ions may be applied externally, i.e., all electrodes confining the collision chamber are kept at the same potential and ions are extracted only by means of a penetrating field produced by electrodes placed beyond the collision chamber exit slit.[47-50] Unfortunately, except for general studies about the influence of the repeller voltage on the ion trajectories which include the limit of the zero repeller voltage,[35,40,41,46,47] no extensive experimental study on these operating conditions has yet been made.

In the present study we found that the latter ion extraction method (no electric field applied inside the collision chamber) is superior to the use of a repeller field,[14,21,22] since this effectively avoids discrimination at the collision chamber exit slit. This will become apparent in the following discussion of our present experimental method (refer to Figs. 2 and 3). The ions produced in the electron beam (electron currents $\lesssim 3$ μA) are drawn out of the collision chamber C through a slit in L_1 (1.5 mm width and about 8 mm height) under the action of the electric field which penetrates into the collision chamber C from lens L_2. Lens L_1 (which is commonly called extraction lens) and the pusher P of our conventional Nier-type three electrode ion source are kept at the potential of the collision chamber C (typically +3 kV), whereas L_2 is kept at +2.7 to 2.85 kV.

Figure 3 gives a schematic illustration of the equipotential lines under these extraction conditions.[47] The arrangement of the collision chamber electrodes is similar to the ion source geometry used by Werner,[41,42] who studied the influence of different ion source parameters on the extraction of ions in a magnetic sector field

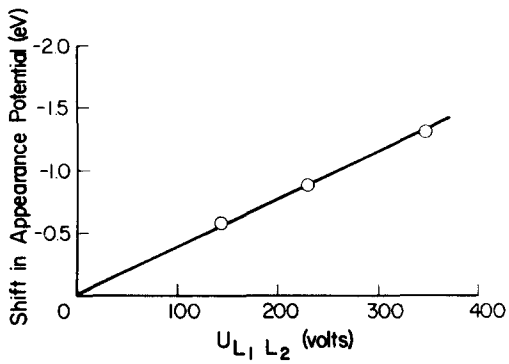

FIG. 6. Shift in measured appearance potential for process $Ar + e \rightarrow Ar^+ + 2e$ as a function of potential difference between L_1 and L_2 ($U_{L_1L_2}$).

mass spectrometer by means of computer calculated ion trajectories. Werner found for the case where the influence of the penetrating field in the extraction region is high compared to the field established by the repeller (and this is close to the present case) that all ions starting within a given region (in our case this region is much greater than the cross section of the electron beam) are extracted through L_1.

The penetrating field will change the energy of the electrons in the ionization region, i.e., it will slow down the electrons when they enter the penetrating field at a and accelerate the electrons to their original velocity when they leave the penetrating field at a' (see Fig. 3). From a shift in the measured appearance potential A.P. (Ar^+) we find that the potential at the position of the electron beam increases nearly linearly with the potential difference $U_{L_1L_2}$, the increase being about 100 mV per 30 V (see Fig. 6). It should be mentioned that the influence of the electric extraction field is found to be much more severe in cases where the electric field is applied between electrodes confining the collision chamber.[22,51,52]

In order to check the efficiency and accuracy of this extraction mode in our experiments, without interference from the mass spectrometer (discrimination at the entrance and exit slits of the mass spectrometer), we first measured in the plane of the mass spectrometer entrance slit the total ion current drawn from the collision chamber. Figure 7 shows that the extracted ion signal indeed saturates if the voltage difference $U_{L_1L_2}$ (which is responsible for the strength of the penetration field) is raised to above 150 V. A small but residual increase in the saturation current is attributed to a continuous but small extension of the ion withdrawal space between a and a'.

This total ion current, measured as a function of electron energy under saturation condition ($U_{L_1L_2} > 150$ V), agrees quite well (within 1%) with the previously measured and well established total ionization cross section curves of Rapp and Englander-Golden.[23] An example of this is shown in Fig. 8 for helium with the following electrode potentials (measured with respect to ground): $P = C = L_1 = 3$ kV, $L_2 = 2.850$ kV, $L_3 = 2.850$ kV, $L_4 = 2.772$ kV, $L_6 = 0.060$ kV, $L_7 = 0.200$ kV, $L_5 = L_8 = L_9 = S_1 = 0$ kV. It

is interesting to note that no such agreement could be achieved if the ions were extracted in the usual way[37,53] under the action of an electric field applied between electrodes inside the collision chamber.[21,22]

Having demonstrated that ion extraction exclusively with a penetrating field is effective, the next step in our investigation was to study the transmission of the extracted ion current through the mass spectrometer. This was done first by measuring the extracted helium ion current in the plane of the mass spectrometer entrance slit S_1, then in the plane of DA, and finally on the Faraday collector F (see Fig. 1). It was found that the transmission is only of the order of a few percent and depends strongly on the potentials applied to the electrodes L_2 to L_5.

In order to find out if the fraction of the ion beam collected after mass analysis at the Faraday collector is representative of the total ion beam extracted from the ion source, we measured the mass analyzed ion current (He^+) as a function of electron energy and as a function of the potential difference $U_{L_1L_2}$. The ion currents obtained as a function of electron energy did not generally agree with the shape of the established total ionization cross section function of He.[23] In helium this comparison is straightforward, because in our electron energy range the total ionization cross section of He is equal to the partial ionization cross section of He^+ within 0.6%. As will be shown later, the reason for this observed discrepancy is a change of the shape of the extracted ion beam with electron energy which results in changing fractions of the ion beam passing the mass spectrometer entrance slit. Moreover, no saturation of the mass analyzed ion current with increasing potential difference $U_{L_1L_2}$ could be observed.[47] The explanation for this effect lies in the fact that lens L_2 not only acts as extraction electrode but also as a focusing electrode, i.e., with increasing potential $U_{L_1L_2}$ the ion beam becomes smaller in size and hence the fraction of ions passing S_1 becomes larger.

It was therefore necessary to examine more closely the ion beam shape at the mass spectrometer entrance slit S_1. The shape of the ion beam under different experimental conditions was determined using two pairs of deflecting electrodes as shown in Figs. 1 and 2 (L_6, L_7, and L_8, L_9). These deflection electrodes allow movement of the fanned-out ion beam past the mass spectrometer entrance slit in the y and z direction (see Fig. 1), thereby enabling a two dimensional analysis of the beam with the mass spectrometer. If the width of the slit is small compared to the extension of the beam, the curve of ion current versus deflection voltage directly gives the shape of the ion beam in one direction.

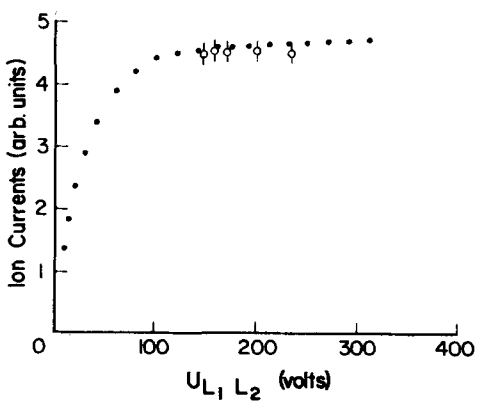

FIG. 7. Ion current as a function of potential difference between L_1 and L_2 for a midpoint potential $U_M = 450$ V. Full dots: total helium ion current measured in the plane of the mass spectrometer entrance slit. Open circles: integrated He^+ ion current (see text).

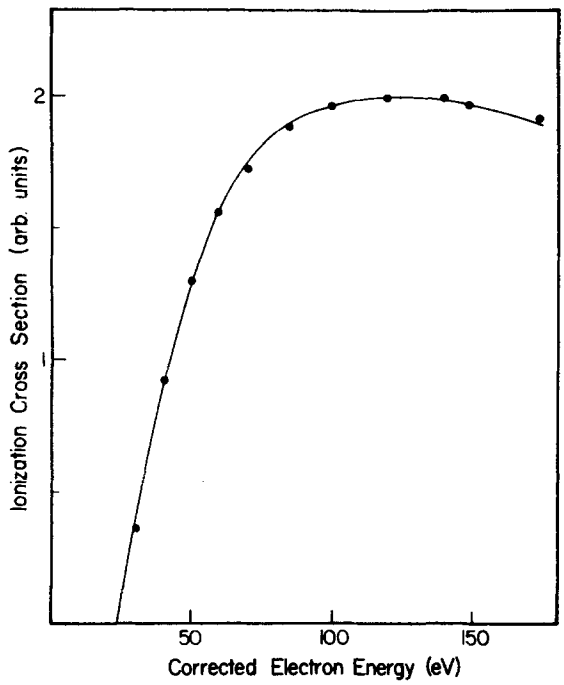

FIG. 8. Ionization cross section versus corrected electron energy. Full dots: total ionization cross sections of He measured by Rapp and Englander-Golden[23] with an ionization tube. Full line: total ion current of He measured in the plane of the mass spectrometer entrance slit normalized to the data of Rapp and Englander-Golden at 100 eV.

For the following it is convenient to define the potential difference between L_1 and the midpoint between L_3 and L_4 as $U_M = U_{L_1} - (U_{L_3} + U_{L_4})/2$. Deflection curves for the y direction for two different midpoint potentials U_M are shown in Figs. 9 and 10. Figure 9 shows the Ar^+ and Ar^{2+} beam profiles in y direction for strong focusing action ($U_M = 425$ V) of the lens L_3 and L_4, On the other hand, using only a weak focusing action ($U_M = 190$ V) results in a much broader flat topped ion beam shape in the y direction (Fig. 10). The area under the deflection curves in both cases (Figs. 9 and 10) should give a representative measure of the total ion flux through the ion source exit slit S_1 for a given m/e. This is because any discrimination at the entrance slit in the y direction is being eliminated by this procedure (neglecting possible losses in the z direction; see below). Typical results of the integrated ion current (He^+) as a function of the potential difference $U_{L_1L_2}$ are shown in Fig. 7 (open circles). It can be seen that the integrated ion currents saturate in the same way as the total ion currents measured in the plane of the mass spectrometer entrance

slit. It is important to note that Coggeshall,[36] who first introduced this method to monitor the ion flux through the mass spectrometer entrance slit, found no saturation for the integrated ion currents as a function of *repeller potential*. This clearly demonstrates the advantage of the present extraction mode, where no repeller field is used.

The principal test of this deflection method, however, was to see whether the measured mass analyzed ion current integrated in the y direction, as a function of electron energy, gives the correct cross section curve. In the case of helium the comparison can be made directly with the total ionization cross section curve. A comparison with the data of Rapp and Englander-Golden[23] showed close agreement (see present results on He^+) and gave us confidence in our approach. At this point it might be worth pointing out that some authors[43,50] attempt to focus the entire ion beam upon the mass spectrometer entrance slit in order to avoid any discrimination at this slit. This is contrary to the present approach, where discrimination at S_1 is avoided by integration over the beam profile. The present approach was adopted, because it was found impossible to transmit the entire ion beam through S_1.

The use of this deflection and integration procedure appears to be impracticable for determining accurate relative partial ionization cross sections, since extremely stable experimental conditions are required over a long time period in order to measure deflection curves at each electron energy. A more direct method of measuring partial ionization cross sections is based on our observation that the ion beam profile shown in Fig. 10 does not change (within ±2%) with electron energy. Hence, centering the beam approximately on the mass spectrometer entrance slit yields a mass analyzed portion of the ion beam which is representative of the total beam profile and therefore the partial ionization cross section. This is due to the fact that, as shown above, the total ion current in plane S_1 is representative

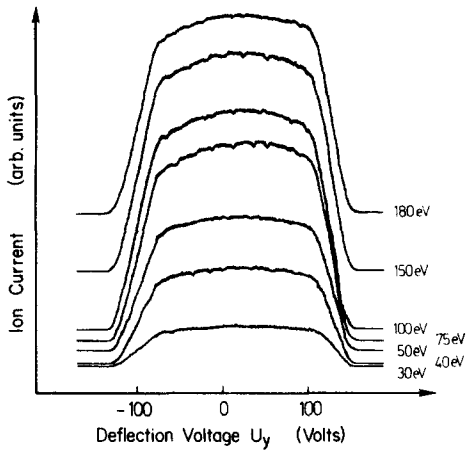

FIG. 10. Deflection curves for Ar^+ ions giving the ion beam profile in the y direction for different electron energies. $U_{L_1L_2} = 150$ V and $U_M = 190$ V.

of the ionization cross section. All relative cross section functions reported in the present study have been measured in this way. The following potentials were used:

$$P = C = L_1 = 3 \text{ kV}, \quad L_2 = 2.850 \text{ kV}, \quad L_3 = 2.819 \text{ kV},$$

$$L_4 = 2.803 \text{ kV}, \quad L_5 = 0 \text{ kV}, \quad L_6 = L_7 = 0.130 \text{ kV}, \quad S_1 = 0 \text{ kV}.$$

So far only properties of the ion beam in the y direction have been considered. However, it is also necessary to explore discrimination in the z direction,[54] especially since the ionic path in the z direction is limited to 6 mm in the magnetic sector field,[55] while the slit S_1 and S_2 accept an ion beam extending 8 mm in the z direction (as compared to a slit width of less than 1 mm). Figures 11 and 12 show ion beam profiles in the z direction for Ar^+ and Ar^{2+} for two different midpoint potentials $U_{M_z} = (U_{L_6} + U_{L_7})/2$. As in the case of the y direction, the shape of the beam in the z direction depends on the applied midpoint potential of the respective electrodes

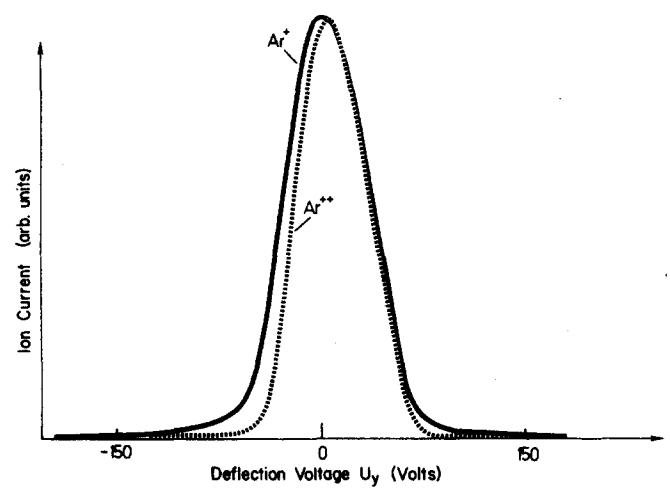

FIG. 9. Deflection curves for Ar^+ and Ar^{2+} giving the ion beam profile in the y direction. The deflection voltage $U_y = U_{L_9} - U_{L_8}$. $U_{L_1L_2} = 340$ V and $U_M = 425$ V.

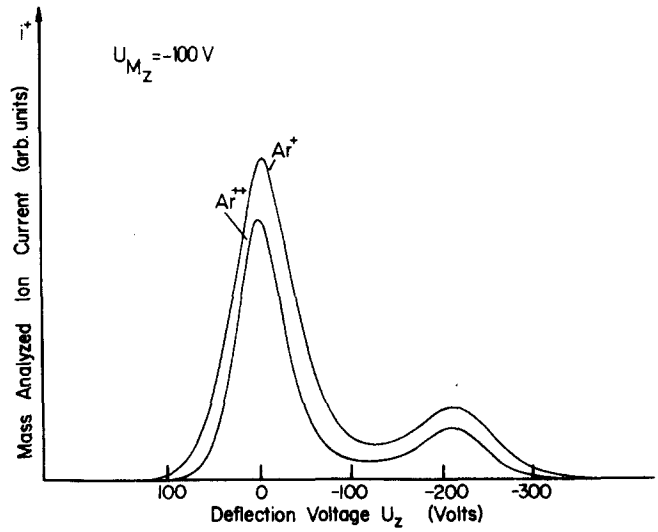

FIG. 11. Deflection curves for Ar^+ and Ar^{2+} giving the ion beam profile in the z direction ($U_{M_z} = -100$ V). The deflection voltage $U_z = U_{L_6} - U_{L_7}$.

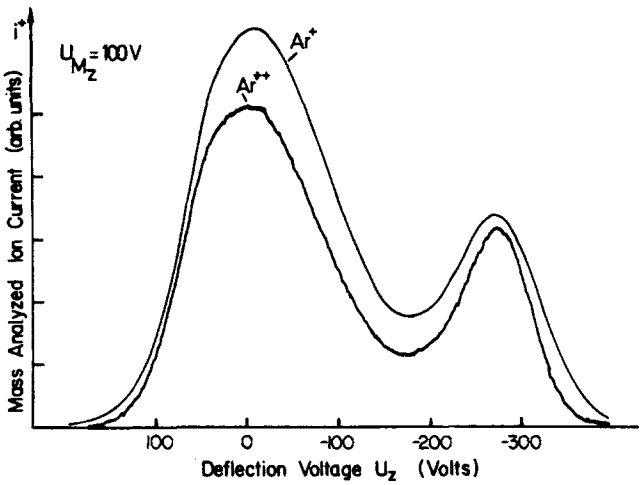

FIG. 12. Same as Fig. 11 but with $U_{M_z} = +100$ V.

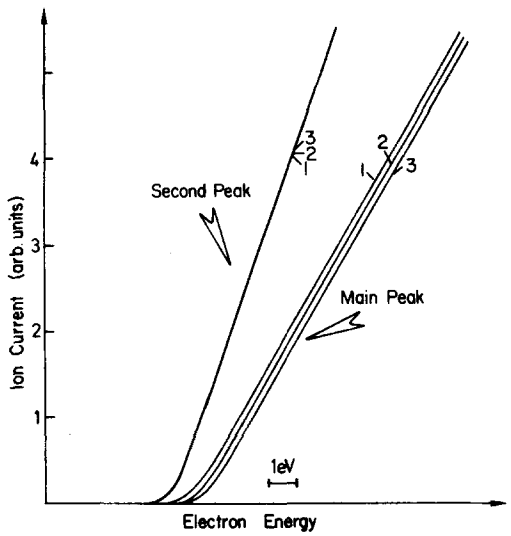

FIG. 14. Ionization efficiency curve close to threshold for He^+ ions of the main peak ($U_z = 0$ V) and of the second peak ($U_z = -200$ V) for the z-deflection curve. Curve (1): $U_{L_1L_2} = 150$ V; curve (2): $U_{L_1L_2} = 235$ V; curve (3): $U_{L_1L_2} = 340$ V. For ions of the second peak the ionization curve does not shift with $U_{L_1L_2}$.

(L_3 and L_4 for y and L_6 and L_7 for z). The presence of a second peak observed in these deflection curves was unexpected.

In order to explain the smaller peak we made further tests. It was found that the position of the smaller peak with respect to the main peak was strongly dependent on the penetrating field, whereas the position of the main peak is independent (see Fig. 13). Moreover, Fig. 14 shows that the appearance potential determined of ions in the small peak is smaller than the appearance potential of ions in the main peak (both peaks refer to mass analyzed He^+ currents). In addition, the appearance potential of ions in the small peak is independent of the strength of the penetrating field. Thus, we conclude ions corresponding to the small peak are produced in a region outside the influence of the penetrating field (e.g., outside of the region a and a' in Fig. 3). The position of the smaller peak indicates that the origin of these ions lies beyond a. We explain the occurrence of this small peak as ionization of gas atoms adsorbed on the collision chamber walls being caused by stray electrons.[56] This is further substantiated by the fact that the *relative* amount of ions within the small peak increases with increasing electron current (see Fig. 15).

This is because focusing conditions of the electron beam become worse with increasing electron current, and relatively more electrons will eventually strike the wall of the collision chamber in the vicinity of the electron beam exit slit (also see Fig. 3).

In conjunction with this problem, it is interesting to report some deflection curves which we obtained in a previous study of the electron impact ionization of neutral rare gas dimers.[25] Figure 16 shows ion beam profiles in the z direction measured for Ar^+ formed in a static gas target in comparison to Ar_2^+ produced from neutral Ar_2 in the molecular beam. It is important to point out, here again, that for the static gas target ionization occurs over the entire electron beam path. In contrast, since the weakly bound neutral dimers are not expected to survive collisions, the neutral dimers available for ionization are present only in a small volume

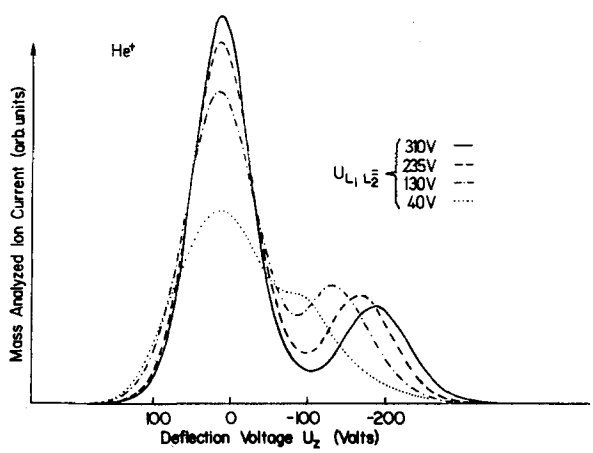

FIG. 13. Same as Fig. 11 but with $U_{L_1L_2}$ as the parameter.

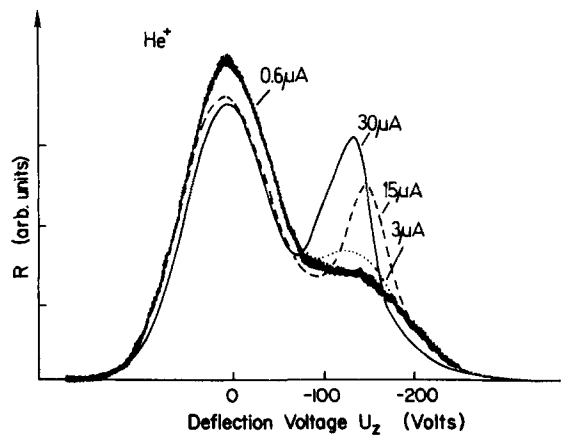

FIG. 15. Ratio of mass analyzed ion current and trap electron current as a function of deflection voltage U_z. Parameter: trap electron current. $U_{L_1L_2} = 130$ V.

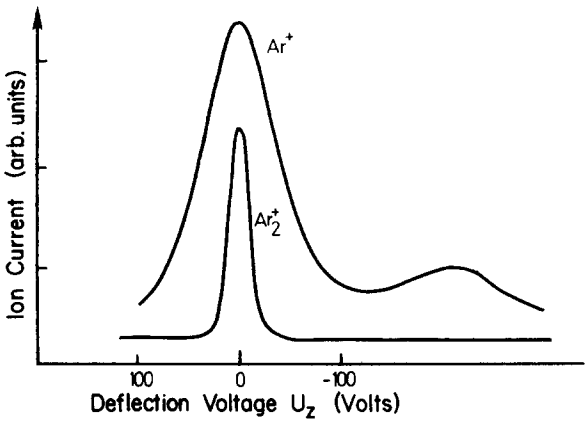

FIG. 16. Deflection curves for Ar^+ and Ar_2^+ giving the ion beam profile in the z direction.

where the molecular beam and electron beam overlap. The latter property causes the beam profile for Ar_2^+ to be narrower than that of Ar^+ from the static gas target. Moreover, the lack of appearance of a second peak in the beam shape of dimer ions is in agreement with the conclusion above, namely, that the second peak originates from interaction of electrons with the wall layer.

In principle, the present integration method has to be applied to both directions in order to monitor the total ion current in front of S_1 from the mass analyzed ion signal. We have therefore taken a series of y deflection curves at various z positions in the ion beam for Ar^+ and Ar^{2+} at an electron energy of 180 eV. Pointwise integration has been used to obtain the current ratio. For example, using $U_{M_z} = +100$ V, a ratio of $i(Ar^{2+})/i(Ar^+) = 0.134$ and at $U_{M_z} = -100$ V a ratio of 0.137 have been obtained. Integrating in the y direction only at a z position in the main peak of the z profile [$U_z = 0$ and $U_{M_z} = +100$ V (the latter condition assures a broad beam profile in the z direction; see Fig. 12)], we obtain a value of the ion current ratio $i(Ar^{2+})/i(Ar^+) = 0.134$. Within the accuracy of the integration method all three values of this ratio are identical. On the other hand, if we do not perform the integration over the y direction, the obtained current ratio shows a systematic dependence on the deflection voltage U_y. This is because the multiply charged ions exhibit a smaller FWHM than singly charged ions of the same gas (see Fig. 9). The origin of the necessity of integrating over the y direction, but not over the z direction, lies in the fact that the ion beam profile emerging from the collision chamber is a band whose height (z extension) is determined by the extension a–a', which is of the order of 15 mm, whereas the width (y extension) is determined by the electron beam waist, which in turn is primarily defined by the width of the electron beam entrance slit (2.8 mm). For the measurements reported in the present paper we have therefore obtained cross section ratios by integration over the y profile only; the dependence of the ion current on electron energy was determined using the conditions given in Fig. 10 (see the discussion above). In order to demonstrate that cross section ratios derived in this way are independent of other instrumental effects, we have varied experimental parameters over a wide range and determined ion current ratios by integration in the y direction. For the example given above [$i(Ar^{2+})/i(Ar^+)$ at 180 eV] the measured current ratios were found to be (1) independent of the penetrating field (in the saturation region), (2) independent of the gas density in the collision chamber (studied pressure range 10^{-6} to 2×10^{-5} Torr, as measured outside of the collision chamber with an ionization gauge), (3) independent of the electron current (for currents below 15 μA [21,22]), (4) independent of the ion accelerating voltage (1, 2, and 3 kV), and (5) independent of the width of the mass spectrometer exit slit. In this context, independence means that the current ratio was within the range 0.136 ± 0.006 with no apparent systematic dependence on the parameters mentioned above.

After all the consistency checks described were made, the only remaining question concerned possible variation of the electron path length with electron energy due to the guiding magnetic field. Rapp and Englander-Golden[23] have shown, for a similar magnetic field strength in a very careful error analysis based on the work of Massey and Burhop[57] and Asundi,[58] that the energy dependence of the total ionization cross sections (measured by them and used in the present paper for comparison) is accurate to better than ±1%. A recent systematic investigation of spiraling in a magnetically confined electron beam confirms that errors are likely to be only a few percent.[59] Therefore, we conclude that path length corrections are quite small in the experiments reported herein; therefore, they are neglected in what follows.

III. RESULTS

After the experimental method described in the previous section was checked in detail, relative partial ionization cross section functions were measured under the proper conditions for the various rare gases. This was done by measuring the electron energy dependence of the cross section for each ion in each gas in a series of runs, in which the electron energy was selected manually on a 10-turn helipot. At each selected electron energy a data acquisition unit recorded the ion current i^+, electron energy, and the gas pressure in the ion source p and in the gas reservoir. Before and after each run the calibration of the pressure gauges was recorded. The ratio $i^+/p(i_t + i_s)$ was determined for each value of electron energy and tabulated using a PDP 11 computer. Typically, in one run a total of ~400 values of this ratio was measured at ~100 different values of the electron energy. A tabulation of the relative cross sections at electron energy intervals of 5 eV is prepared by the computer program by means of linear interpolation of several sets of data points for each cross section curve.

Special care was taken in the absolute calibration of the electron energy scale. The relative electron energy, obtained by reading the electron accelerating voltage applied, needs to be calibrated because of the influence of (1) contact potentials between the electron gun electrodes, (2) the penetrating field, and (3) the electron energy spread introduced by the hot filament. As has been pointed out by Märk and de Heer,[60] this calibration

TABLE I. Partial ionization cross section ratios of the electron impact production of multiply to singly ionized rare gas ions at three different electron energies.

Cross section ratio	Electron energy 50 eV	100 eV	150 eV	Reference
$\frac{q(He^{2+}/He)}{q(He^{+}/He)}$	...	...	0.0025	Bleakney and Smith[7]
	...	0.00040	0.0021	Fox[62]
	...	0.00037	0.0020	Adamczyk *et al.*[9]
	...	0.0025	0.0040	Gaudin and Hagemann[38]
	...	0.00030	0.0023	Egger and Märk[2]
	...	0.00038	0.0020	Present study
$\frac{q(Ne^{2+}/Ne)}{q(Ne^{+}/Ne)}$	...	0.017	0.041	Bleakney[5]
	...	0.010	0.034	Adamczyk *et al.*[9]
	...	0.022	0.039	Gaudin and Hagemann[38]
	...	0.013	0.038	Egger and Märk[2]
	...	0.009	0.029	Present study
$\frac{q(Ar^{2+}/Ar)}{q(Ar^{+}/Ar)}$	0.014	0.10	0.11	Bleakney[5]
	0.007	0.10	0.10	Stevenson and Hipple[8]
	0.009	0.10	0.087	Fox[63]
	...	0.087	0.088	Fiquet-Fayard and Lahmani[65,66]
	...	0.071	0.064	Peterson[68]
	...	0.079	...	Melton and Rudolph[70]
	...	0.050	0.066	Gaudin and Hagemann[38]
	0.004	0.050	...	Morrison and Traeger[71]
	0.005	0.070	0.073	Crowe *et al.*[10]
	...	0.070	...	Drewitz[11]
	0.008	0.084	0.086	Egger and Märk[2]
	0.0064	0.068	0.071	Present study
$\frac{q(Ar^{3+}/Ar)}{q(Ar^{+}/Ar)}$	...	0.0003	0.0014	Fox[63]
	...	0.0005	0.0026	Fiquet-Fayard and Lahmani[65,66]
	...	<0.0035	...	Melton and Rudolph[70]
	...	0.0009	0.0022	Gaudin and Hagemann[38]
	...	0.00028	...	Drewitz[11]
	...	0.00059	0.0037	Egger and Märk[2]
	...	0.0003	0.0019	Present study
$\frac{q(Kr^{2+}/Kr)}{q(Kr^{+}/Kr)}$	0.03	0.12	0.12	Tate and Smith[6]
	0.04	0.15	0.14	Fox[63]
	0.03	0.15	0.14	Ziesel[68]

TABLE I (*Continued*)

Cross section ratio	Electron energy 50 eV	100 eV	150 eV	Reference
$\frac{q(Kr^{2+}/Kr)}{q(Kr^{+}/Kr)}$	0.030	0.12	0.11	Egger and Märk[2]
	0.028	0.087	0.087	Present study
$\frac{q(Kr^{3+}/Kr)}{q(Kr^{+}/Kr)}$	...	0.0025	0.010	Tate and Smith[6]
	...	0.0037	0.013	Fox[63]
	...	0.0032	0.010	Ziesel[68]
	...	0.0027	0.010	Egger and Märk[2]
	...	0.0018	0.0065	Present study
$\frac{q(Xe^{2+}/Xe)}{q(Xe^{+}/Xe)}$	0.10	0.17	0.14	Tate and Smith[6]
	0.12	0.28	0.28	Fox[62,63]
	0.76	0.15	0.15	Egger and Märk[2]
$\frac{q(Xe^{3+}/Xe)}{q(Xe^{+}/Xe)}$	...	0.026	0.063	Tate and Smith[6]
	...	0.050	0.089	Fox[62,63]
	...	0.025	0.069	Egger and Märk[2]
$\frac{q(Xe^{4+}/Xe)}{q(Xe^{+}/Xe)}$	...	...	0.004	Tate and Smith[6]
	...	...	0.003	Fox[62,63]
	...	...	0.005	Egger and Märk[2]

is of great importance when cross section curves of different authors are compared at low electron energies. In the present study a crucial test was the comparison with the data of Rapp and Englander-Golden.[23] Thus, the energy scale was established by plotting for each gas the singly charged ion current versus electron energy and extrapolating linearly to threshold. The same procedure was applied to the data of Rapp and Englander-Golden[23]; the potential difference between our apparent appearance potential and their determined appearance potential was subtracted from our relative nominal electron energy. This method assures optimum agreement between both energy scales. The applicability of the linear extrapolation method, necessary for this calibration, has been confirmed previously.[24] Rapp and Englander-Golden[23] have calibrated their energy scale by plotting the electron current versus electron energy and extrapolating to zero electron current, thus obtaining an absolute energy scale. Cross checks carried out by Rapp and Englander-Golden with various gases have resulted in good agreement with well established appearance potential values in all cases.

Relative partial ionization cross section functions from threshold up to 180 eV electron energy have been measured for the following processes:

$$\mathrm{He} + e \rightarrow \begin{cases} \mathrm{He}^{+} + 2e\,, \\ \mathrm{He}^{2+} + 3e\,, \end{cases}$$

$$\mathrm{Ne} + e \rightarrow \begin{cases} \mathrm{Ne}^{+} + 2e\,, \\ \mathrm{Ne}^{2+} + 3e\,, \\ \mathrm{Ne}^{3+} + 4e\,, \end{cases}$$

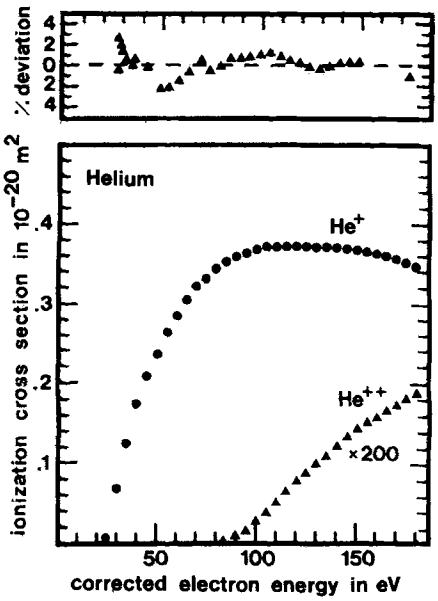

FIG. 17. Upper part: The ratio of the total ionization cross sections for He between the present results and the data of Rapp and Englander-Golden.[23] Lower part: Absolute partial ionization cross sections versus electron energy for the processes $He + e \rightarrow He^+ + 2e$ and $He + e \rightarrow He^{2+} + 3e$.

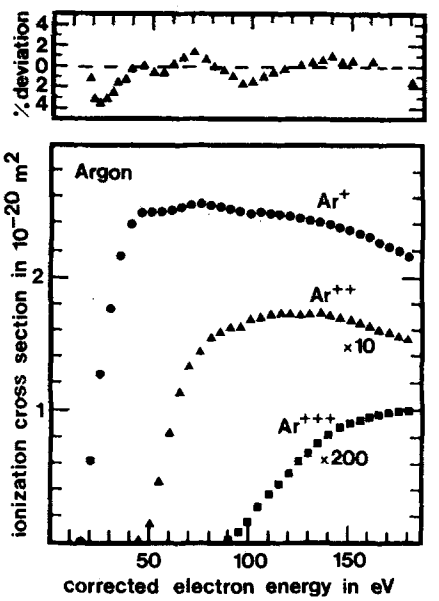

FIG. 19. Upper part: The ratio of the total ionization cross sections for Ar between the present results and the data of Rapp and Englander-Golden.[23] Lower part: Absolute partial ionization cross sections versus electron energy for the processes $Ar + e \rightarrow Ar^+ + e$, $Ar + e \rightarrow Ar^{2+} + 3e$, and $Ar + e \rightarrow Ar^{3+} + 4e$.

$$\text{Ar} + e \rightarrow \begin{cases} \text{Ar}^+ + 2e\,, \\ \text{Ar}^{2+} + 3e\,, \\ \text{Ar}^{3+} + 4e\,, \end{cases}$$

$$\text{Kr} + e \rightarrow \begin{cases} \text{Kr}^+ + 2e\,, \\ \text{Kr}^{2+} + 3e\,, \\ \text{Kr}^{3+} + 4e\,, \\ \text{Kr}^{4+} + 5e\,, \end{cases}$$

In addition, we also measured cross section ratios for all ions within each gas at several electron energies. The maximum statistical deviations for the measured cross section ratios are at 150 eV: ± 4% for Ne^{2+}/Ne^+, Ar^{2+}/Ar^+, and Kr^{2+}/Kr^+; ~ ± 7% for He^{2+}/He^+, Ar^{3+}/Ar^+, and Kr^{3+}/Kr^+; ~ ± 18% for Ne^{3+}/Ne^+ and Kr^{4+}/Kr^+. The results of these measurements are given in Table I. Using these measured cross section ratios, it is possible

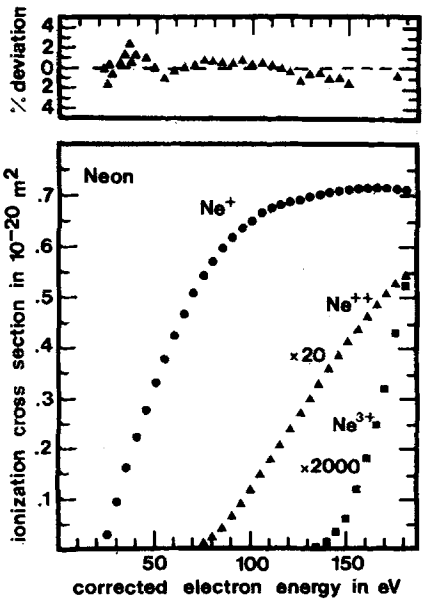

FIG. 18. Upper part: The ratio of the total ionization cross sections for Ne between the present results and the data of Rapp and Englander-Golden.[23] Lower part: Absolute partial ionization cross sections versus electron energy for the processes $Ne + e \rightarrow Ne^+ + 2e$, $Ne + e \rightarrow Ne^{2+} + 3e$, and $Ne + e \rightarrow Ne^{3+} + 4e$.

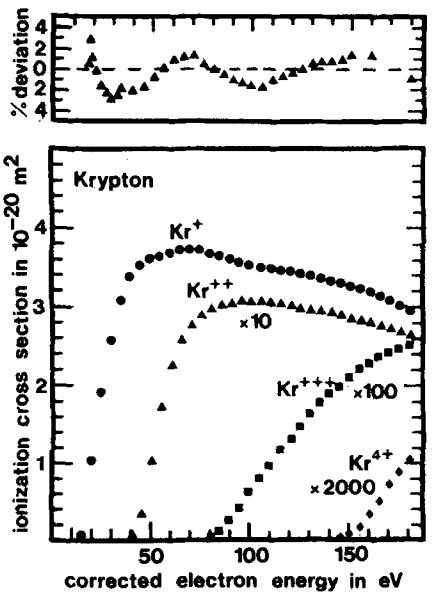

FIG. 20. Upper part: The ratio of the total ionization cross sections for Kr between the present results and the data of Rapp and Englander-Golden.[23] Lower part: Absolute partial ionization cross sections versus electron energy for the processes $Kr + e \rightarrow Kr^+ + 2e$, $Kr + e \rightarrow Kr^{2+} + 3e$, $Kr + e \rightarrow Kr^{3+} + 4e$, and $Kr + e \rightarrow Kr^{4+} + 5e$.

TABLE II. Absolute partial ionization cross sections versus electron energy for the processes $He + e \rightarrow He^+ + 2e$ and $He + e \rightarrow He^{2+} + 3e$.

Electron energy (eV)	$q(He^+/He)$ (10^{-20} m^2)	$q(He^{2+}/He)$ (10^{-24} m^2)
25	0.007	
30	0.069	
35	0.125	
40	0.175	
45	0.210	
50	0.237	
55	0.265	
60	0.286	
65	0.306	
70	0.323	
75	0.333	
80	0.344	
85	0.354	0.1
90	0.360	0.5
95	0.365	0.8
100	0.369	1.4
105	0.373	2.0
110	0.374	2.6
115	0.374	3.3
120	0.374	4.0
125	0.373	4.4
130	0.372	5.0
135	0.372	5.6
140	0.372	6.0
145	0.371	6.7
150	0.369	7.2
155	0.367	7.6
160	0.364	8.0
165	0.362	8.4
170	0.358	8.7
175	0.353	9.1
180	0.349	9.4

to calibrate the relative partial ionization cross section functions within each gas against each other. The sum of these calibrated cross section functions, each weighted with the charge number, gives a relative total ionization cross section function. The shape of the total ionization cross section curve, thus obtained from our mass spectrometric measurements, can be compared with ionization tube measurements of the total ionization cross section curve. These latter values had been determined *without* mass analysis. Such a comparison has been made with the well established[1,60,61] data of Rapp and Englander-Golden[23] and is plotted for each gas in the upper part of Figs. 17–20. It can be seen that the overall agreement is within a few percent.

This comparison of total ionization cross section curves allows an absolute normalization of the relative partial ionization cross section functions. The absolute partial ionization cross section functions obtained in this manner are shown in the lower part of Figs. 17–20 and are tabluated in Tables II–V for He, Ne, Ar, and Kr, respectively.

Errors in the energy dependence of the cross sections arise from two sources. One is the statistical error, caused by purely random changes in the measured ion current. This error could be estimated by taking frequent repeat measurements of the cross section at some fixed energy. The reproducibility at the maximum of the cross section was usually $\sim \pm 2\%$ for He^+, Ne^+, Ar^+, and Kr^+; $\sim \pm 3\%$ for Ne^{2+}, Ar^{2+}, and Kr^{2+}; $\sim \pm 8\%$ for He^{2+}, Ar^{3+}, and Kr^{3+}; and $\sim \pm 12\%$ for Ne^{3+} and Kr^{4+}. Systematic errors, on the other hand, can only be surmised from various empirical tests. We have shown in Sec. II that systematic errors due to discrimination in the ion extraction and transmission should be quite small. In attempting to determine limits of the systematic errors it is possible to use the comparison of total cross sections discussed above (the relative accuracy of the data of Rapp and Englander-Golden being better than $\pm 1\%$). It can be seen that the agreement of our mass spectrometer data with the total ionization apparatus data[23] is within the combined statistical error.

The absolute normalization of the cross sections is subject to considerably larger errors due to errors in the measured cross section ratios and the unknown error in the absolute total ionization cross sections of Rapp and Englander-Golden.[23] The estimated error of the absolute partial ionization cross sections at their maximum, excluding the unknown error of the total ion-

TABLE III. Absolute partial ionization cross sections versus electron energy for the processes $Ne + e \rightarrow Ne^+ + 2e$, $Ne + e \rightarrow Ne^{2+} + 3e$, and $Ne + e \rightarrow Ne^{3+} + 4e$.

Electron energy (eV)	$q(Ne^+/Ne)$ (10^{-20} m^2)	$q(Ne^{2+}/Ne)$ (10^{-20} m^2)	$q(Ne^{3+}/Ne)$ (10^{-24} m^2)
25	0.037		
30	0.102		
35	0.169		
40	0.230		
45	0.284		
50	0.337		
55	0.386		
60	0.432		
65	0.475		
70	0.513	0.0002	
75	0.549	0.0006	
80	0.576	0.0013	
85	0.602	0.0021	
90	0.623	0.0033	
95	0.642	0.0046	
100	0.655	0.0059	
105	0.670	0.0074	
110	0.683	0.0090	
115	0.690	0.0105	
120	0.696	0.0122	
125	0.697	0.0138	
130	0.706	0.0152	
135	0.708	0.0167	
140	0.711	0.0182	
145	0.714	0.0195	0.2
150	0.717	0.0208	0.4
155	0.718	0.0220	0.6
160	0.720	0.0233	0.9
165	0.722	0.0244	1.3
170	0.720	0.0255	1.6
175	0.720	0.0266	2.2
180	0.717	0.0274	2.6

TABLE IV. Absolute partial ionization cross sections versus electron energy for the processes $Ar + e \rightarrow Ar^+ + 2e$, $Ar + e \rightarrow Ar^{2+} + 3e$, and $Ar + e \rightarrow Ar^{3+} + 4e$.

Electron energy (eV)	$q(Ar^+/Ar)$ (10^{-20} m^2)	$q(Ar^{2+}/Ar)$ (10^{-20} m^2)	$q(Ar^{3+}/Ar)$ (10^{-23} m^2)
20	0.61		
25	1.26		
30	1.76		
35	2.15		
40	2.39		
45	2.49	0.001	
50	2.49	0.016	
55	2.49	0.045	
60	2.50	0.082	
65	2.52	0.113	
70	2.54	0.133	
75	2.54	0.144	
80	2.53	0.154	
85	2.52	0.159	
90	2.51	0.162	0.11
95	2.49	0.162	0.33
100	2.46	0.168	0.74
105	2.47	0.170	1.35
110	2.47	0.171	1.75
115	2.46	0.172	2.19
120	2.45	0.173	2.64
125	2.44	0.172	3.07
130	2.42	0.172	3.39
135	2.40	0.173	3.73
140	2.40	0.171	4.04
145	2.37	0.170	4.28
150	2.35	0.167	4.46
155	2.32	0.165	4.63
160	2.30	0.162	4.73
165	2.25	0.160	4.79
170	2.23	0.158	4.89
175	2.19	0.156	4.89
180	2.15	0.153	4.95

ization cross section of Ref. 23, is ~±3% for He^+, Ne^+, Ar^+, and Kr^+; ~±10% for Ne^{2+}, Ar^{2+}, and Kr^{2+}; ~±18% for He^{2+}, Ar^{3+}, and Kr^{3+}; and ±33% for Ne^{3+} and Kr^{4+}.

In summarizing the error analysis, it should be pointed out once more that the confidence in the accuracy given for our data stems primarily from two facts: (1) the extensive study of possible systematic errors in the extraction and transmission mechanism and (2) the good agreement between our total ionization cross sections and those of ionization tube measurements.

IV. DISCUSSION

The data available on partial ionization cross section functions and ratios of the rare gases are summarized in Ref. 1 and more recently in Ref. 2 for electron energies < 180 eV. There are essentially three different types of data that have been reported, i.e., *relative* partial ionization cross section functions,[6–8,10,62,63,65–67,69,70,72] *absolute* partial ionization cross section functions,[5,9,38,66,71] and partial cross section *ratios*.[2,6–8,10,11,62–64,66,67,69,70,72] Because of differences in the absolute normalization (the crux is obviously the difference in total cross section values used for the normalization), it is not meaningful to compare absolute values of the present results of the partial cross section functions. Rather, attention must be focused on their shape and/or their relative abundances compared with those of previous determinations.

The data available on partial ionization cross section ratios are summarized in Table I. Some of the previous data on cross section ratios were measured using electron multipliers as detectors, without taking into account that the secondary electron response is affected by the energy and type of the impinging ion.[73–75] These data have not been included in Table I. This is because cross section ratios measured with uncalibrated multipliers cannot be considered as reliable as direct measurements using a Faraday cup, except where ion counting is employed which effectively calibrates[1] the multiplier used.[10,64,71]

Of the experiments presented in Table I, only those of Adamczyk *et al.*,[9] Crowe *et al.*,[10] and Drewitz[11] employ methods which ensure similar extraction and transmission efficiencies for ions of different charge (see also discussion in Sec. II). Adamczyk *et al.*[9] have used a cycloidal mass spectrometer, which does not suffer

TABLE V. Absolute partial ionization cross sections versus electron energy for the processes $Kr + e \rightarrow Kr + 2e$, $Kr^+ + e \rightarrow Kr^{2+} + 3e$, $Kr + e \rightarrow Kr^{3+} + 4e$, and $Kr + e \rightarrow Kr^{4+} + 5e$.

Electron energy (eV)	$q(Kr^+/Kr)$ (10^{-20} m^2)	$q(Kr^{2+}/Kr)$ (10^{-20} m^2)	$q(Kr^{3+}/Kr)$ (10^{-20} m^2)	$q(Kr^{4+}/Kr)$ (10^{-24} m^2)
15	0.23			
20	1.23			
25	2.05			
30	2.69			
35	3.14			
40	3.41	0.004		
45	3.53	0.035		
50	3.60	0.101		
55	3.63	0.171		
60	3.68	0.226		
65	3.70	0.257		
70	3.72	0.277		
75	3.69	0.290		
80	3.66	0.298	0.0003	
85	3.62	0.302	0.0011	
90	3.57	0.304	0.0027	
95	3.53	0.306	0.0042	
100	3.50	0.305	0.0063	
105	3.47	0.305	0.0080	
110	3.47	0.304	0.0096	
115	3.45	0.301	0.0115	
120	3.42	0.300	0.0132	
125	3.40	0.296	0.0147	
130	3.38	0.294	0.0163	
135	3.35	0.292	0.0189	0.02
140	3.31	0.289	0.0199	0.21
145	3.28	0.284	0.0210	0.48
150	3.25	0.281	0.0221	0.90
155	3.20	0.280	0.0225	1.31
160	3.17	0.279	0.0229	1.73
165	3.13	0.275	0.0236	2.55
170	3.07	0.271	0.0241	3.64
175	3.02	0.267	0.0246	4.45
180	2.96	0.266	0.0251	5.22

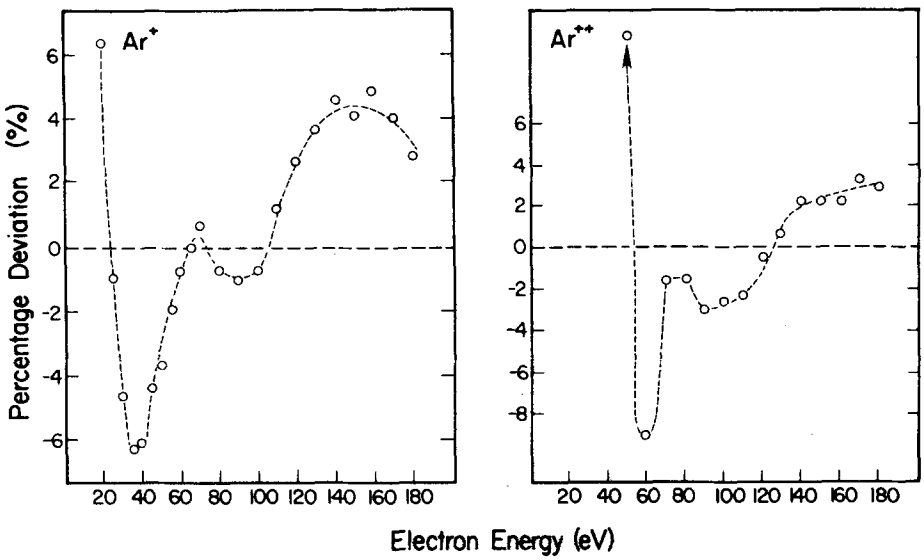

FIG. 21. The ratio of the partial ionization cross sections for the processes $Ar + e \rightarrow Ar^+ + 3e$ and $Ar + e \rightarrow Ar^{2+} + 3e$ between the present results and the data of Crowe, Preston, and McConkey.[10]

the drawback of m/e dependent collection efficiency. The mass spectrometer employed in their study did not have slits in the ion source, and the authors claim that it is possible to attain a complete collection of all ions produced in the source. They report absolute partial ionization cross sections for He^+, He^{2+}, Ne^+, Ne^{2+}, and Ne^{3+}. Their results on the cross section ratios He^{2+}/He^+ and Ne^{2+}/Ne^+ agree quite well with the present results (see Table I), which in turn is further evidence for the reliability of the data on ionization cross sections presented in this paper.

Crowe *et al.*[10] have recently carried out studies on the ionization of Ar in which they have taken great care to fulfill the requirements outlined by Kieffer and Dunn[1] for the accurate measurement of ionization efficiencies. Their apparatus consisted of a modified Pierce-type electron gun which produced a beam of electrons with an extremely small beam divergence over the complete energy range studied (<300 eV). The ions which were generated in a field free region were allowed to drift through two apertures that defined the angular resolution of the system before being accelerated and focused into a quadrupole mass spectrometer. Care was taken to ensure that the ratio Ar^{2+}/Ar^+ was independent of the mass spectrometer resolution used. The mass analyzed ions were detected using a channeltron multiplier in conjunction with pulse counting. Measurements were made for a configuration of 90° between the electron beam and detection system, and Crowe *et al.*[10] demonstrated that the angular distributions of Ar^+ and Ar^{2+} were independent of the electron energy. The cross section ratios Ar^{2+}/Ar^+ deduced from their results at 50, 100, and 150 eV electron energy agree well with the present results (see Table I). Crowe *et al.*[10] compared their ionization curve obtained for Ar^+ with various previous results normalized to their data at 50 eV and found good agreement in shape between their curve and that of Bleakney.[5] However, their curve does indicate a structure in the region just above 50 eV. They do not explain this structure in terms of "competition" theory,[3] but instead suggest that the double maximum is caused by processes whose maximum probability occurs at different energies. The most likely secondary process is shown to be autoionization. Despite the fact that all three curves indicate structure above 50 eV, the results of Morrison and Traeger,[72] Fiquet-Fayard,[65] and of Stevenson and Hipple[8] are generally in strong disagreement with the data of Crowe *et al.*[10] The results of Fox,[63] which are strongly dependent on his experimental conditions, and similar data by Stuber[69] are also in very poor agreement with the data of Crowe *et al.*[10]

As can be seen from Fig. 19, the present results confirm the existence of structure in the Ar^+ curve as reported by Crowe *et al.*[10] Figure 21 shows a comparison between the results of Crowe *et al.*[10] and the present curves obtained for Ar^+ and Ar^{2+}. The overall agreement between the two sets of measurements is within a few percent except close to threshold. This could be due to differences in the electron energy scale calibration, which may lead to large discrepancies close to threshold.[60]

Drewitz[11] has recently reported cross section ratios for argon at 100 eV electron energy. He eliminated the effect of discrimination at the mass spectrometer exit (collector) slit of his 60° sector field mass spectrometer by monitoring the z profile of the ion beam behind the mass spectrometer entrance slit.[28,76-78] In addition, Drewitz and Taubert[43] tried to eliminate the discrimination caused by the mass spectrometer entrance slit with help of a focal lens situated between the collision chamber exit slit and the mass spectrometer entrance slit. The cross section ratios Ar^{2+}/Ar^+ and Ar^{3+}/Ar^+ reported by Drewitz[11] both agree well with the present results.

Early work on electron impact ionization of rare gases had been made with an instrument devised by Bleakney ney,[5,79] which employed for the first time a magnetically collimated beam of electrons transverse to the ion beam. The entire apparatus (180° deflection type analyzer and the ion source) was placed within a solenoid which produced the requisite magnetic field strength. In the apparatus used by Tate and Smith[6] the long slits used in Bleakney's apparatus are replaced by slits of ~0.5 mm length. An apparatus similar to that of Tate and Smith[6]

was used by Stevenson and Hipple[8] and by Bleakney and Smith.[7] In all of these cases the ions were accelerated through a first slit by a field applied between electrodes *inside* the ion source; they enter the mass analyzer through a second slit. Thus, in accordance with previous findings concerning discrimination effects during extraction and transmission,[21,22,27-29,33-36,39-46] the cross section functions and cross section ratios reported in Refs. 5–8 are expected to be subject to systematic errors.[1] It can be seen from Table I that cross section ratios reported by Bleakney,[5] Tate and Smith,[6] Bleakney and Smith,[7] and Stevenson and Hipple[8] are all considerably higher for the rare gases than the present values. However, differences in the shape of relative cross section functions between their results and our curves are less than the differences in cross section ratios.

Fox[62,63] has measured relative partial ionization cross section functions and partial cross section ratios for He, Ar, Kr, and Xe. His experiments were performed with a 90° sector field type mass spectrometer, but no detailed information on the ion source operation is available. The reported relative ionization curves and cross section ratios of Fox[62,63] strongly disagree with the present results. As mentioned by Fox, his results were dependent on experimental conditions and it was difficult to eliminate instrumental effects. Comparisons of the ionization efficiency curves of Ne, Ar, Kr, and Xe published by Stuber[70] obtained with a Bendix time-of-flight mass spectrometer show similarities with the results obtained by Fox.[62,63] The peculiar very low second maxima in the Ar^+ and Kr^+ curves were also observed by Stuber.[70] Differences between Stuber's curves and those published in other previous studies are attributed by Stuber to experimental factors.

Stanton and Monohan[64] report measurements of the ratio of He^+ and He^{2+} yields for electron energies between 100 and 2400 eV with an energy selecting 60° sector field mass spectrometer. Their graphical representation of data at 100 and 150 eV electron energy does not allow a meaningful comparison with our data. Hence, their results are not included in Table I.

Fiquet-Fayard, Lahmani, and Ziesel[65-67,69] have published several studies concerning the electron impact ionization of Ar and Kr for an electron energy range up to 2000 eV. They measured cross section ratios and a relative cross section function using a 60° sector field analyzer and a Nier-type ion source without a magnetic guiding field. In their first study[65] they used a repeller field to extract ions out of the ion source and observed that the shape of the measured Ar ionization efficiency curves was strongly dependent on the repeller field applied.[21,22] In their latter studies[66,67,69] they extracted the ions in a similar way as in the present study. The curves obtained for Kr under the more recent experimental conditions agree reasonably well with the present ionization cross section functions. However, cross section ratios derived from their data[65,66,69] are considerably higher than the present results (Table I).

Gaudin and Hagemann[38] have made a detailed study of the electron impact ionization of He, Ne, and Ar. Using a Nier-type ion source with repeller and a 90° sector field mass analyzer, they measured absolute total and partial ionization cross section functions and cross section ratios from 100 to 2000 eV. Mass analyzed ion signals were measured using a Faraday cup. They measured ion current abundances by choosing ion source operation conditions for maximum transmission of the singly charged ion. To demonstrate their accuracy, they showed that ion current ratios change only slightly with ion accelerating voltage. However, it should be noted that both cross section ratios and functions may suffer from instrumental effects if the Nier source is operated in this way.[21,22] A comparison of the cross section ratios shows that their values deviate strongly from the present results, i.e., their ratios are smaller for Ar, whereas they are larger for He and Ne.

Melton and Rudolph[71] have determined partial and total ionization cross sections of Ar at 100 eV electron energy with a dual electron beam ion source[80,81] in conjunction with a 60° sector field instrument. They only give an upper limit for the cross section of Ar^{3+} at 100 eV; their cross section ratio Ar^{2+}/Ar^+ is slightly larger than the present value.

Morrison and Traeger[72] have measured relative partial cross section functions, and the corresponding cross section ratio of Ar^+ and Ar^{2+} using a quadrupole mass filter with an electron multiplier detector.[82] They argue that because the dependence of sensitivity on m/e for the electron multiplier is canceled by the dependence of the transmission efficiency of the quadrupole, the ratio measured for Ar^{2+}/Ar^+ is, to a good approximation, what would be expected for a magnetic sector analyzer and a Faraday cup detector. Their measured cross section ratios, however, disagree with the present results, and, as has been mentioned above, also their Ar^+ cross section curve strongly disagrees with the present data and those of Crowe *et al.*[10]

Egger and Märk[2] have recently measured the cross section ratios of the rare gases with an experimental set up similar to that described in the present paper. The authors were aware of discrimination effects at the collision chamber exit slit and mass spectrometer entrance slit. They measured ionization efficiency curves as a function of the applied extraction and focusing potentials, and found that cross section curves and ratios depend strongly on the extraction condition. In order to obtain cross section ratios they carried out an averaging procedure giving cross section ratios with an estimated systematic error of 10% to 20%. As can be seen from Table I, their values agree with the present ones to within the limits of the combined error.

Finally, it is interesting to note that Peterson[68] and more recently Brook *et al.*[83] have used a quite different approach to study electron impact ionization cross section functions. It employs a crossed-beam arrangement, wherein the target beam of neutral atoms (He, Ne, Ar) is obtained from a fast ion beam by charge transfer. Absolute cross sections for different charge states are obtained directly without measurements of gas pressure or temperature. However, as pointed out by Peterson, the method has attractive advantages as well as its own

difficulties and problems. The cross section ratios Ar^{2+}/Ar^{+} reported by Peterson[68] are close to the present values (Table I), although there are discrepancies in the shape of the cross section functions (Ne^{+}, Ne^{2+}, Ar^{+}, and Ar^{2+}) between the results of Peterson and the present ones. If an electron energy scale correction is applied to their data,[60] the cross sections for ionization of He reported by Brook *et al.*[83] are seen in good agreement with the present data.

V. CONCLUSION

A new approach to mass spectrometric measurement and analysis has been used in these studies. We carried out careful consistency checks on the extraction and collection efficiency of ions. We report partial ionization cross section functions and cross section ratios for He, Ne, Ar, and Kr. Because of the improvements in the technique and the precautions taken in acquiring the data, we believe that the reported energy dependence of partial ionization cross sections and the cross section ratios belong to the most accurate ionization cross sections measured with a mass spectrometer.

ACKNOWLEDGMENTS

The authors are grateful to the Österreichischer Fonds zur Förderung der Wissenschaftlichen Forschung for financial assistance under Project No. S-18|08. It is a pleasure to acknowledge partial support by the Cooperative Institute for Research in Environmental Sciences (CIRES), University of Colorado/NOAA, Boulder, Colorado. We would like to thank Professor A. W. Castleman, Jr., Department of Chemistry, University of Colorado, Boulder, for critically reading the manuscript.

[1]L. J. Kieffer and G. H. Dunn, Rev. Mod. Phys. **38**, 1 (1966).
[2]F. Egger and T. D. Märk, Z. Naturforsch. Teil A **33**, 1111 (1978).
[3]D. Rapp, J. Chem. Phys. **55**, 4154 (1971).
[4]C. Lifshitz, J. Chem. Phys. **55**, 4155 (1971).
[5]W. Bleakney, Phys. Rev. **36**, 1303 (1930).
[6]J. T. Tate and P. T. Smith, Phys. Rev. **46**, 773 (1934).
[7]W. Bleakney and L. G. Smith, Phys. Rev. **49**, 402 (1936).
[8]D. P. Stevenson and J. A. Hipple, Phys. Rev. **62**, 237 (1942).
[9]B. Adamczyk, A. J. H. Boerboom, B. L. Schram, and J. Kistemaker, J. Chem. Phys. **44**, 4640 (1966).
[10]A. Crowe, J. A. Preston, and J. W. McConkey, J. Chem. Phys. **57**, 1620 (1972).
[11]H. J. Drewitz, Int. J. Mass Spectrom. Ion Phys. **19**, 313 (1976); **21**, 212 (1976).
[12]F. Egger, thesis, Universität Innsbruck, 1977.
[13]E. Hille, thesis, Universität Innsbruck, 1979.
[14]K. Stephan, thesis, Universität Innsbruck, 1979.
[15]T. D. Märk, F. Egger, E. Hille, M. Cheret, H. Störi, and K. Stephan, Proceedings of the Xth International Conference on the Physics of Electronic and Atomic Collisions, Paris (1977), p. 1070.
[16]E. Hille, T. D. Märk, and H. Störi, Proceedings of the 1st Symposium on Atomic and Surface Physics, Tirol (1978), p. 59.
[17]K. Stephan, T. D. Märk, and H. Helm, Proceedings of the 1st Symposium on Atomic and Surface Physics, Tirol (1978), p. 77.
[18]K. Stephan, H. Helm, and T. D. Märk, Proceedings of the IXth Symposium on the Physics of Ionized Gases, Dubrovnik (1978), p. 7.
[19]H. Helm, K. Stephan, and T. D. Märk, 31st Gaseous Electronics Conference, Buffalo (1978).
[20]K. Stephan, H. Helm, and T. D. Märk, Proceedings of the 8th International Mass Spectrometry Conference, Oslo (1978); Adv. Mass Spectrometry, **8** (1980).
[21]T. D. Märk and A. W. Castleman, Proceedings of the 2nd Symposium on Atomic and Surface Physics, Salzburg (1980), p. 146; and J. Phys. E **13** (1980).
[22]K. Stephan, E. Hille, H. Helm, and T. D. Märk (to be published).
[23]D. Rapp and P. Englander-Golden, J. Chem. Phys. **43**, 1464 (1965).
[24]T. D. Märk, J. Chem. Phys. **63**, 3731 (1975); T. D. Märk and F. Egger, Int. J. Mass Spectrom. Ion Phys. **20**, 89 (1976); T. D. Märk and F. Egger, J. Chem. Phys. **67**, 2629 (1977); T. D. Märk, F. Egger, and M. Cheret, J. Chem. Phys. **67**, 3795 (1977); T. D. Märk and E. Hille, J. Chem. Phys. **69**, 2492 (1978); E. Hille and T. D. Märk, J. Chem. Phys. **69**, 4600 (1978).
[25]H. Helm, K. Stephan, and T. D. Märk, Phys. Rev. A **19**, 2154 (1979).
[26]A. O. Nier, Phys. Rev. **50**, 1041 (1936); **52**, 933 (1937).
[27]E. B. Jordan and N. D. Coggeshall, J. Appl. Phys. **13**, 539 (1942).
[28]C. E. Berry, Phys. Rev. **78**, 597 (1950).
[29]H. D. Hagstrum and J. T. Tate, Phys. Rev. **59**, 354 (1941).
[30]A. O. Nier, Rev. Sci. Instrum. **11**, 212 (1940).
[31]N. D. Coggeshall and E. B. Jordan, Rev. Sci. Instrum. **14**, 125 (1943).
[32]R. L. Graham, A. L. Harkness, and H. G. Thode, J. Sci. Instrum. **24**, 119 (1947).
[33]N. D. Coggeshall, J. Chem. Phys. **12**, 19 (1944).
[34]O. A. Schaeffer, Rev. Sci. Instrum. **25**, 660 (1954).
[35]R. Vauthier, Ann. Phys. (Paris) **10**, 968 (1955).
[36]N. D. Coggeshall, J. Chem. Phys. **36**, 1640 (1962).
[37]R. M. Elliot, in *Mass Spectrometry*, edited by C. A. McDowell (McGraw-Hill, New York, 1963), p. 72.
[38]A. Gaudin and R. Hagemann, J. Chim. Phys. **64**, 1209 (1967).
[39]W. Schulz, H. Drost, and H. D. Klotz, Exp. Tech. Phys. **16**, 16 (1968).
[40]M. J. Wallington, J. Phys. E **4**, 1 (1971).
[41]H. W. Werner, J. Phys. E **7**, 115 (1974).
[42]H. W. Werner, Int. J. Mass Spectrom. Ion Phys. **14**, 189 (1974).
[43]H. J. Drewitz and R. Taubert, Int. J. Mass Spectrom. Ion Phys. **19**, 293 (1976).
[44]H. W. Washburn and C. E. Berry, Phys. Rev. **70**, 559 (1946).
[45]P. S. Naidu and K. O. Westphal, Brit. J. Appl. Phys. **17**, 653 (1966).
[46]W. Fock, Int. J. Mass Spectrom. Ion Phys. **3**, 285 (1969).
[47]J. Chantreau and R. Vauthier, *Recent Developments in Mass Spectroscopy* (University Park, Baltimore, 1970), p. 198.
[48]W. Paul, Z. Phys. **124**, 244 (1948).
[49]A. O. Nier, Rev. Sci. Instrum. **18**, 398 (1947).
[50]H. D. Hagstrum, Rev. Mod. Phys. **23**, 185 (1951); Rev. Sci. Instrum. **24**, 1122 (1953).
[51]R. E. Honig, J. Chem. Phys. **16**, 105 (1948).
[52]J. D. Waldron and K. Wood, *Mass Spectrometry* (Institute of Petroleum, London, 1952), p. 16.
[53]C. Brunnee and H. Voshage, *Massenspektrometrie* (Thiemig, München, 1964).
[54]It should be noted that Berry[28] and Drewitz and Taubert[43] used a similar method, however, applying the z-deflection field after and not before the mass spectrometer entrance slit.
[55]The limitation is caused by the dimensions of the vacuum

tubing between the pole shoes of the magnetic sector field.
[56]We base this tentative conclusion on the following argument: A single monolayer of adsorbed atoms represents an apparent density of approximately 10^{22} atoms per cm^3 to an electron beam transversing the monolayer. Despite the small thickness of the layer of adsorbed atoms, the effective target thickness of the wall layer is for one monolayer about 300 times greater than the target thickness seen by the electron beam in the volume of the collision chamber at a pressure of 10^{-5} Torr. Requiring that only ~1% of the ions formed in the uppermost monolayer are able to escape from the wall, we can account for the observed abundance of the ions in the second peak in Figs. 11–14. We are currently investigating this phenomenon in more detail.
[57]H. S. W. Massey and E. H. S. Burhop, *Electronic and Ionic Impact Phenomena* (Oxford University, New York, 1952).
[58]R. K. Asundi, Proc. Phys. Soc. London **82**, 372 (1963).
[59]P. O. Taylor, K. T. Dolder, W. E. Kauppila, and G. H. Dunn, Rev. Sci. Instrum. **45**, 538 (1974).
[60]T. D. Märk and F. J. de Heer, J. Phys. B **12**, L429 (1979).
[61]F. J. de Heer, R. H. J. Hansen, and K. van der Kaay, J. Phys. B **12**, 979 (1979).
[62]R. E. Fox, J. Chem. Phys. **33**, 200 (1960).
[63]R. E. Fox, *Advances in Mass Spectrometry*, edited by S. D. Waldron (Pergamon, London, 1953), pp. 397.
[64]H. E. Stanton and J. E. Monahan, J. Chem. Phys. **119**, 711 (1960).
[65]F. Fiquet-Fayard, J. Chim. Phys. **59**, 439 (1962).
[66]F. Fiquet-Fayard and M. Lahmani, J. Chim. Phys. **59**, 1050 (1962).
[67]F. Fiquet-Fayard and J. P. Ziesel, Proceedings of the VIth International Conference on the Physics of Ionized Gases, Paris (1963), p. 37.
[68]J. R. Peterson, *Atomic Collision Processes*, edited by M. R. C. McDowell, Proceedings of the 3rd ICPEAC, London, 1963 (North Holland, Amsterdam, 1964), p. 465; and private communication (1980).
[69]J. P. Ziesel, J. Chim. Phys. **64**, 695 (1967).
[70]F. A. Stuber, Chem. Phys. **42**, 2639 (1965).
[71]C. E. Melton and P. S. Rudolph, J. Chem. Phys. **47**, 1771 (1967).
[72]J. D. Morrison and J. C. Traeger, J. Chem. Phys. **53**, 4053 (1970).
[73]B. L. Schram, A. J. H. Boerboom, W. Kleine, and J. Kistemaker, Physica (Utrecht) **32**, 749 (1966).
[74]M. Van Gorkom and R. E. Glick, Int. J. Mass Spectrom. Ion Phys. **4**, 203 (1970).
[75]T. D. Märk, Z. Naturforsch. Teil A **32**, 1559 (1977).
[76]R. M. Reese and J. A. Hipple, Phys. Rev. **75**, 1332 (1949).
[77]D. Osberghaus and R. Taubert, Angew. Chem. **63**, 287 (1951).
[78]R. Taubert, Z. Naturforsch. Teil A **19**, 484 (1963).
[79]W. Bleakney, Phys. Rev. **34**, 157 (1929); **35**, 139 (1930).
[80]C. E. Melton, J. Sci. Instrum. **43**, 927 (1966).
[81]C. E. Melton, J. Chem. Phys. **45**, 4414 (1966).
[82]J. D. Morrison (private communication, 1976).
[83]E. Brook, M. F. A. Harrison, and A. C. H. Smith, J. Phys. B **11**, 3115 (1978).